RAPID COMMUNICATIONS

PHYSICAL REVIEW E VOLUME 49, NUMBER 5 MAY 1994

Average patterns in Faraday waves

Eric Bosch, Hans Lambermont, and Willem van de Water
Physics Department, Eindhoven University of Technology, P.O. Box 513, 5600 MB Eindhoven, The Netherlands
(Received 13 December 1993)

Disordered waves at the surface of a vertically oscillated fluid layer have a nontrivial time average. Using an image-reduction scheme we study the surface dynamics that leads to this average state. We show that the average state arises because wave maxima move erratically but are attracted to the nodes of a lattice. This lattice does not correspond to a simple linear eigenmode of the surface. Both the surface dynamics and the appearance of the average state strongly depend on the boundary condition.

PACS number(s): 47.52.+j, 47.35.+i, 47.54.+r

Spatiotemporal chaos is a property of systems that display disordered behavior both in space and time. It may be a precursor to turbulence that has hierarchical spatial disorder. In spatiotemporally chaotic systems, however, there is often only one wavelength that dominates. Although the number of degrees of freedom is large in these systems, they do allow a description in terms of parameters of their phase space, such as the dimension or the Lyapunov exponents. A challenge is to find possibly universal relations between real-space and phase-space quantities [1]. So far, this problem has been addressed in the context of numerical experiments where both real-space and phase-space quantities are available. However, the practical measurement of phase-space quantities in experiments already encounters grave problems when the number of degrees of freedom is only moderately large.

In two recent papers [2,3] it was found that for spatiotemporally chaotic systems the measurement of a very simple quantity, the time-averaged state, produces highly nontrivial results. While snapshots of the system showed a disordered pattern, the average state has the symmetry of the pattern before the order-disorder transition. How these patterns were formed was not well understood, but it was found that the correlation of instantaneous patterns with the average strongly fluctuates and is biased towards positive values. Also, the contrast of the averaged state decays when the system is more strongly driven. In [3] it was shown that this effect depends on the system size or aspect ratio. This is the ratio of the system size L to the basic wavelength λ of the pattern. For small values of L/λ the boundary is important and the system adapts its global state to the boundary condition, yielding a nonflat average state. As the aspect ratio becomes large, the average state becomes flat, except in a small region near the boundary.

The experiments in this paper concern capillary waves on the surface of a vertically oscillated fluid [4,5]. These waves are formed at a critical excitation amplitude $\mathcal{A}_c$ through a parametric instability. For amplitudes $\mathcal{A}$ just above $\mathcal{A}_c$ there is a stationary wave pattern. As will be discussed later, this pattern depends on the type of boundary condition. The pattern becomes time dependent and disordered for larger reduced amplitudes $\epsilon = (\mathcal{A} - \mathcal{A}_c)/\mathcal{A}_c$. In agreement with Gluckman *et al.* [2], we also find that the average of the surface in the disordered regime is not flat. In the present paper we will concentrate on the surface dynamics that gives rise to the average state.

An interesting aspect of our experiment is the reduction of shadowgraph images of the surface to the set of their local intensity maxima. This is a crucial data reduction scheme that enables us to study the dynamics of the surface over many thousands of snapshots. We will show that this technique provides superior insight into the nature of the average state.

Our experiment consists of a square container with side $L = 80$ mm filled to a level of 10 mm with a low viscosity silicon oil [6]. The excitation frequency was $f = 81.7$ Hz yielding an aspect ratio $L/\lambda = 17$. We measure the amplitude interferometrically with a relative accuracy of 2×10^{-4}. The temperature is kept constant at $T = 294.00 \pm 0.03$ K. The control of the excitation amplitude and the acquisition of images is automated allowing for long unattended runs. This enables scans of the control parameter ϵ, registering 3000 images at each ϵ setting. The surface waves were visualized by shining a parallel beam of light through the bottom of the container, resulting in a shadowgraph image on a translucent screen attached to the top.

The images of the surface were digitized using a 1024×1024 8-bit noninterlaced charge-coupled device (CCD) camera connected to a real-time image processing system. The camera is tightly synchronized with the experiment. Images of the surface were integrated over one quarter of the wave period (half the drive period), synchronized to the phase of the surface waves. The algorithm that reduced images to the positions of the wave maxima [7] yields a data reduction by a factor of 5000 (depending on the number of wave maxima found) and enables us to store thousands of images for each value of the driving amplitude. The maximum sample frequency achieved is 2.5 Hz, allowing us to actually follow the wave maxima at moderate excitation amplitudes ($\epsilon < 0.6$). Finding wave maxima is not always unambiguous, especially for the high values of ϵ where the patterns are highly disordered and wave antinodes are continuously created and annihilated.

The planar geometry of our container is square but we have tried various boundary conditions in the vertical direction. At one extreme the boundary was steplike with

the fluid surface level with the step. Although a small meniscus was present, this boundary effectively pinned the fluid surface. Just above onset, each linear mode $\zeta(x,y) = \zeta_0(\sin\frac{\pi n}{L}x \sin\frac{\pi m}{L}y + \sin\frac{\pi m}{L}x \sin\frac{\pi n}{L}y)$ with $n = 34$ and $m = 1$–8 could be obtained by fine-tuning the frequency.

At the other extreme the boundary is a vertical wall to which the fluid attaches via a meniscus. Due to this meniscus this boundary is "free" and there is no frequency selectivity as for the "pinned" boundary. The free boundary gives, just above onset, a square pattern in the center of the container under an angle of 45° with the wall. This state obviously does not correspond to any linear eigenmode of the system. The pattern becomes more aligned and more space-filling with increasing amplitude until it is completely lined up with the wall at the order-disorder transition [8]. Below the threshold for Faraday waves, waves emitted by the meniscus are observed at the excitation frequency. It was already noted by Gluckman *et al.* [2] that the "pinned" boundary condition has the clearest average surface state in the disordered regime. However, for reasons discussed below, this boundary troubled the reproducibility of repeated ϵ scans; the reproducibility being superior for the free boundary. The results of these low aspect ratio experiments crucially depend on the boundary condition chosen.

The two types of boundaries give qualitatively different scenarios when ϵ is increased. This is most easily seen when we plot the (horizontal) rms velocity of wave maxima as a function of ϵ. This velocity u was measured by linking wave maxima in two successive images and dividing their displacement by the time interval [9]. The result is shown in Fig. 1.

For the free boundary there is a discontinuous jump from an almost stationary state to a moving state at $\epsilon = \epsilon_c$. In Fig. 1 there is an apparent hysteresis between up and down scans of ϵ. This hysteresis is an experimental artifact and can be made arbitrarily small by increasing the waiting time between amplitude settings. The jump is discontinuous to within the resolution of our amplitude setting. This discontinuous phase transition is different from earlier results [10] for the high aspect ratio, circular cell where the phase transition appears to be continuous.

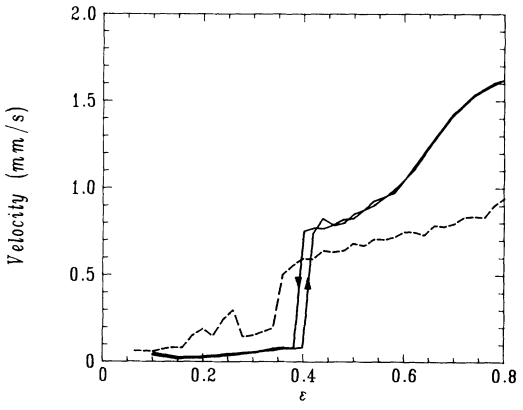

FIG. 1. rms velocity of wave maxima as a function of the excitation amplitude ϵ. Full lines: "free" boundary condition where the fluid surface joins a vertical wall through a meniscus; dashed lines: "pinned" boundary condition. The excitation frequency is 81.7 Hz; images were taken at 2.0425 Hz.

For the pinned boundary the transition is much more complicated. The behavior is strongly dependent on the history and hardly reproducible. In Fig. 1 one typical result is shown. In other pinned boundary experiments (not shown here) the low ϵ behavior differed while the behavior of $u(\epsilon)$ for $\epsilon > \epsilon_c$ was comparable. The "pinned" boundary has a much smaller rms velocity in this regime than the "free" boundary, in agreement with the qualitative observation that the surface fluctuates much more rapidly in the latter case. Finally, a completely pinned boundary was produced using again a steplike boundary that smoothly joined the vertical wall. For this boundary the pattern remained stationary up to $\epsilon = 1.4$. The conclusion is that the transition at $\epsilon = \epsilon_c$ at these small aspect ratios is extremely dependent upon the boundary condition.

In Fig. 2 we show time-averaged states for the "free" boundary. In our representation, the time-averaged state is a superposition of sets of wave maxima from 3000 snapshots. These average pictures are very spiky compared to ordinary averaged images [2]. The comparison, however, is not proper; ordinary averages should be close to a low-pass filtered version of Fig. 2. Our representation clearly illustrates the nature of the nontrivial average. In

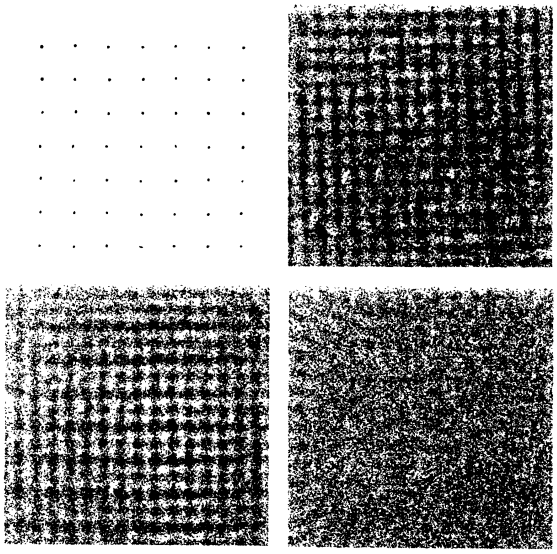

FIG. 2. Average patterns for the "free" boundary condition. The reduced excitation amplitude ϵ is 0.40 for the upper left, 0.42 for the upper right, 0.58 for the lower left, and 0.80 for the lower right image, respectively. The images are taken from a square 35.1 × 35.1 mm^2 section of the cell. The capillary wavelength is $\lambda = 4.71$ mm. At $\epsilon = 0.40$ the pattern is stationary; for clarity the small dots of the stationary lattice have been manually fattened. The distance between the points corresponds to the capillary wavelength. Note the dramatic change of the average as ϵ is increased from $\epsilon = 0.40$ to 0.42.

the disordered state, wave maxima are scattered over the surface but have a tendency to cluster into a new lattice, with half the wavelength of the original lattice. This tendency (cf. the contrast in the picture) becomes weaker for increasing ϵ. We calculate the contrast by filtering the picture using a cutoff low-pass filter (cutoff wavelength $\lambda_c = 0.3\lambda$). The contrast is then the rms intensity variation in the filtered image. Figure 3 shows the dependence of the contrast on ϵ. For the "free" boundary the contrast decays to a small value with increasing excitation amplitude, while the contrast for the "pinned" boundary remains high, even for the highest excitation amplitudes.

Figure 4 shows time-averaged correlation functions $C(x, y)$ of the surface at the same parameter settings as those in Fig. 2. The function $C(x, y)$ is the average of correlation functions computed over single snapshots. In our representation, the correlation function is the histogram of distances between points in a snapshot and accordingly can be calculated very quickly. The result in Fig. 4 is coded in a logarithmic gray scale.

One striking feature is the presence of the basic wavelength even at the highest amplitude. Wave maxima are never closer than this basic wavelength. Furthermore, the patterns seem to have a preferred orientation parallel to the sidewalls (which are also parallel to the picture axes). There is a tendency for the correlations to become more fluidlike (i.e., independent of orientation) towards higher amplitudes. Just above the phase transition the patterns are slightly tilted with respect to the boundary. The tilt angle shows no simple dependence on ϵ and can have both positive and negative values. Above $\epsilon \approx 0.6$ the average patterns are again lined up with the boundary.

The correlation functions show long-range correlation along the axes and much shorter range correlation on the diagonals. This implies that there are narrow bands in both directions that are highly coherent. A visual inspection of the surface shows that the main type of distortions in the disordered state are phase jumps along a line parallel to the boundary, thus maintaining high correlation parallel to the boundary and destroying correlation along the diagonals. At the smallest values of ϵ the wave maxima remain close to the positions of the stationary lattice but undergo random motion. The correlation function

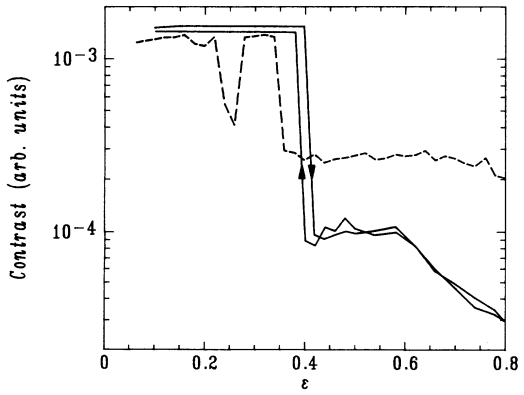

FIG. 3. Contrast of the average patterns as a function of excitation amplitude ϵ. Full lines: "free" boundary condition; dashed lines: "pinned" boundary condition.

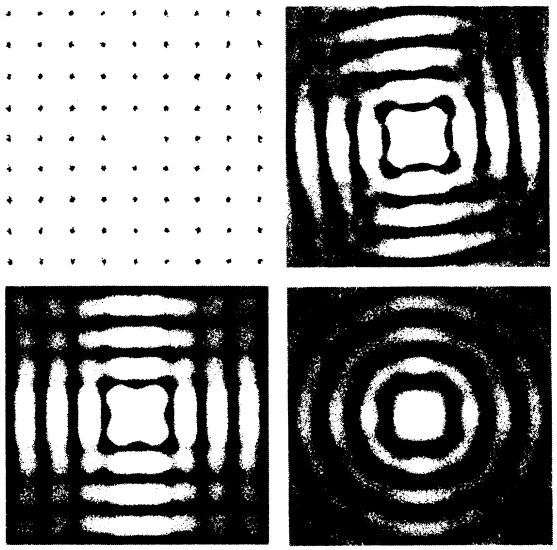

FIG. 4. Time-averaged correlation functions for the free boundary condition and the same values of the amplitude as in Fig. 2. Displacement zero corresponds to the center of the image; the maximum displacement is approximately half the size of the images in Fig. 2. The correlation function is coded in a logarithmic gray scale.

shows that this random motion is uncorrelated at different lattice sites. There is a striking analogy with a thermally excited two-dimensional lattice, but nodal velocities are not Gaussian and preferably directed along the boundaries.

A key observation is that the average surface state in the disordered regime *does not correspond* to a single linear eigenmode of the surface. Since the wavelength in the averaged state is half the wavelength of the stationary state one might be tempted to conclude that the averaged state corresponds to the eigenmode $\zeta(x, y) = \zeta_0(\sin \frac{\pi n}{L} x \sin \frac{\pi n}{L} y)$ with $n = 34$. However, this eigenmode exists at a much higher excitation frequency. Instead, the average pattern is a superposition of the four states $\zeta(x, y) = \zeta_0(\pm \sin \frac{\pi n}{L} x \sin \frac{\pi m}{L} y \pm \sin \frac{\pi m}{L} x \sin \frac{\pi n}{L} y)$ with $n = 34$ and $m = 1$. The superposition of these four states accounts for the half wavelength in the averages. In our case this superposition is nonzero due to the fact that only maxima are detected. In ordinary averages (as in [2]) the nonzero result is due to the nonlinear imaging. We note that changing both signs simultaneously is the same as changing the *temporal* phase by π. This would go unnoticed in experiments where the acquisition of images is not phase locked as in [2]. In the case of the "pinned" boundary the mode selected near the critical amplitude $\mathcal{A}_c$ is one of the four mentioned states with the signs selected at random [11].

In conclusion, we have found that wave maxima move randomly in the disordered surface, but tend to cluster near the nodes of a square lattice. This lattice does *not* correspond to a simple linear eigenmode of the surface. It acts as a state of minimal potential energy. Near onset ($\mathcal{A} = \mathcal{A}_c$) it can attract any of four possible initial square states. Our data of Fig. 4 also suggest that, in

the disordered state, coherence is maintained along lines parallel to the boundaries, but not as a square lattice.

Our work on averages of chaotic patterns has, much as other work [2], been inspired by the ideas of symmetric chaos [12]. One of the key phenomena in symmetric chaos is the occurrence of symmetry increasing bifurcations. The transition to the superposition state is an example of such a bifurcation; the translation symmetry is increased after the transition. Unlike in certain model systems [12], however, this bifurcation coincides with the order-chaos transition.

Clearly the appearance of the average and the surface dynamics that lead to this average do strongly depend on the boundary. A nonflat average will only exist if the boundaries matter. We have found that the average is flat at large aspect ratios ($L/\lambda \simeq 40$). A precise control of the boundary condition is a problem in the Faraday experiment. Therefore experiments with large aspect ratio are preferred, also because they are closer to the thermodynamic limit. However, in this case the average state is flat. We believe that other, long time averaged, quantities are more relevant in this case.

We are deeply indebted to Ludger Welie, who skillfully programmed our real-time image acquisition system. We also thank Professor Gregory King, who convinced us of the relevance of averages.

[1] W. van de Water and T. Bohr, Chaos **3**, 747 (1993).

[2] B.J. Gluckman, P. Marcq, J. Bridger, and J.P. Gollub, Phys. Rev. Lett. **71**, 2034 (1993).

[3] L. Ning, Y. Hu, R.E. Ecke, and G. Ahlers, Phys. Rev. Lett. **71**, 2216 (1993).

[4] M.Faraday, Phil. Trans. R. Soc. London **121**, 319 (1831).

[5] M.C. Cross and P.C. Hohenberg, Rev. Mod. Phys. **65**, 851 (1993).

[6] The silicon oil has at 294 K a viscosity of $\eta = 2.82$ cP, density $\rho = 885\ \mathrm{kg\,m^{-3}}$, and a surface tension $\alpha = 18.3 \times 10^{-3}\ \mathrm{N\,m^{-1}}$.

[7] Image processing involves correction for nonuniform background illumination followed by smoothing the image with a 7×7 kernel. Next pixels are sought that have higher illumination levels than their four nearest neighbors. Only pixels that have an illumination level above a certain threshold are kept. This gives for each wave maximum a (small) cluster of pixels. The location of the center of mass of this set is computed and stored. The only parameter in this algorithm is the intensity of the maximum sought. The results do not depend very much on the precise value taken for the threshold. In practice it is chosen low enough to detect all maxima in the stationary state and high enough to prevent the detection of spurious maxima.

[8] J.P. Gollub and R. Ramshakar, in *New Perspectives in Turbulence*, edited by S. Orszag and L. Sirovich (Springer-Verlag, New York, 1991).

[9] Associating points in two snapshots is subtle. The most important problem is the fact that antinodes may be created or annihilated in between successive snapshots. We search for association of points in two successive snapshots by minimizing the distance between associated points. By introducing a maximum distance l over which a point may travel in between two images we are able to cure this problem. We have verified that our results were essentially the same for any choice of l in the range $\lambda/2$–λ. For high ϵ the lifetime of individual antinodes is so short that an accurate association is no longer possible.

[10] E. Bosch and W. van de Water, Phys. Rev. Lett. **70**, 3420 (1993).

[11] One other candidate for the smaller wavelength would be the meniscus wave pattern which could still influence the Faraday waves. It was verified that the wavelength of the averaged pattern does not correspond to the wavelength of the waves arising from the meniscus, thus ruling out this option.

[12] P. Chossat and M. Golubitsky, Physica D **32**, 423 (1988).

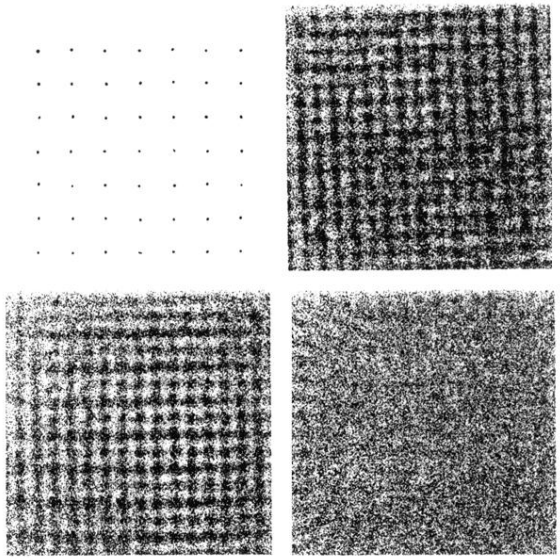

FIG. 2. Average patterns for the "free" boundary condition. The reduced excitation amplitude ϵ is 0.40 for the upper left, 0.42 for the upper right, 0.58 for the lower left, and 0.80 for the lower right image, respectively. The images are taken from a square 35.1×35.1 mm^2 section of the cell. The capillary wavelength is $\lambda = 4.71$ mm. At $\epsilon = 0.40$ the pattern is stationary; for clarity the small dots of the stationary lattice have been manually fattened. The distance between the points corresponds to the capillary wavelength. Note the dramatic change of the average as ϵ is increased from $\epsilon = 0.40$ to 0.42.

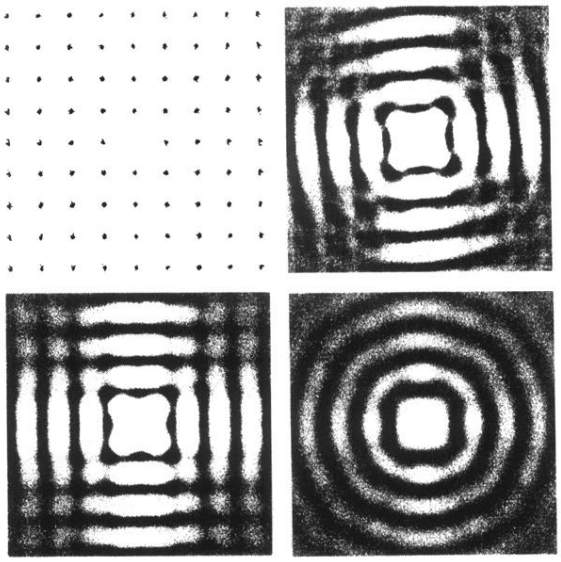

FIG. 4. Time-averaged correlation functions for the free boundary condition and the same values of the amplitude as in Fig. 2. Displacement zero corresponds to the center of the image; the maximum displacement is approximately half the size of the images in Fig. 2. The correlation function is coded in a logarithmic gray scale.